

Computational analysis of peroxisome proliferator-activated receptor-gamma as a nutraceutical target

Stephanie N. Lewis^{1,2,3}, Zulma Garcia², Lera Brannan², Amir J. Guri³, Pinyi Lu^{1,3}, Raquel Hontecillas³, Josep Bassaganya-Riera^{1,3}, and David R. Bevan^{1,2}

¹Genetics, Bioinformatics, and Computational Biology Program,

²Department of Biochemistry, 201 Engel Hall, Virginia Tech,

³Nutritional Immunology and Molecular Medicine Lab, Virginia Bioinformatics Institute, Washington Street 0477 Blacksburg, VA 24061

Abstract

Modulation of the chronic inflammation phenotype associated with many diseases, including diabetes, gastrointestinal diseases, and some cancers, can be attributed to targeting a single family of proteins: peroxisome proliferator-activated receptors (PPAR). With emphasis on PPAR-gamma, we propose using a time- and cost-effective combined computational and experimental approach to screen natural compounds for PPAR-gamma agonists to treat or prevent onset of chronic inflammation-related diseases. Supplementation of the diet with fatty acids, which are known low-level endogenous PPAR-gamma agonists, drives anti-inflammatory and pro-homeostatic mechanisms. Current synthetic drugs for treating chronic inflammation-related diseases are associated with a high incident of side effects, and natural products may be a feasible alternative means of treatment with potential for reduction in harmful effects. Thus far, we identified alpha-eleostearic acid as an ameliorant of inflammatory bowel disease (IBD). Molecular docking and dynamics were used for ligand screening and protein structure analysis; assays and an animal study of pre-clinical efficacy were used to assess in vitro and in vivo effects. Testing, data mining, and expansion of our method to maximize predictability are underway to identify additional potential drug candidates. As part of this expansion we have significantly increased our test compound library, incorporated structural analyses from dynamics simulations to shed light on structural differences induced by ligand binding, and included multiple target structures for docking to accommodate different ligand types. Future work will include implementation of an interaction-based pose scoring system for separating ligand types. Our method allows for testing of diverse ligand datasets against a notoriously difficult docking target, and serves as a first step in improving discovery of beneficial anti-inflammatory natural products. Research support: NIH Biomedical and Behavioral Sciences Research Training Grant R25 GM072767, NCCAM Grant 5R01AT4308, GBCB fellowship (Virginia Tech).

Introduction

Successful treatments for immune-mediated diseases have been shown to target the nuclear hormone receptor peroxisome proliferator-activated receptor-gamma (PPAR γ), which is highly expressed in adipose tissue, colonic epithelium, and immune cells (Dubuquoy et al. 2006. *Gut*. 55). Diseases in which PPAR γ has been proposed to play a role include type 2 diabetes, inflammatory bowel disease, and cancers (e.g., colorectal). PPAR γ is known to play a role in transcriptional regulation of anti-inflammatory processes via co-activator recruitment. This recruitment is directly influenced by ligand binding. Our group has conducted several preclinical animal model studies to suggest that supplementation of diet with fatty acids, is effective at ameliorating inflammation in mouse and pig models through a PPAR γ -dependent mechanism (Bassaganya-Riera et al. 2004. *Gastroenterology*. 127; Bassaganya-Riera et al. 2006. *Clinical Nutrition*. 25). In an effort to expedite the drug and nutraceutical discovery process, virtual screening can complement traditional experimental methods for identification of novel PPAR γ agonists.

Goal: Learn more about PPAR γ as a therapeutic target to facilitate the use of virtual screening to identify novel natural agonists within a collective of large compound databases.

Significance: PPAR γ is a notoriously difficult target for docking studies as numerous crystal structures exist with slight yet significant differences in binding cavity conformation governed by ligand binding. Docking success can be improved by assessing these differences and identifying characteristics key to identifying each ligand type.

Methods

Preliminary screening has indicated that a single PPAR γ structure model would not be sufficient for large-scale screening given binding cavity differences between crystal structures. Techniques for pharmacophore modeling were proposed as a means to assign unknown ligands to specific structure models for screening. Dynamic differences that influence ligand binding were assessed using principal components analysis (PCA). Criteria for successful docking assessment need to be established, which was facilitated by steered molecular dynamics (SMD). AutoDock4 (Morris et al. 1998. *J. Comp. Chem*. 19), Autodock Tools 1.4.5 (Sanner. 1999. *J. Mol. Graphics Mod*. 17) were used for docking. Gromacs 4.0.7 was used for MD (van der Spoel et al. 2005. *J. Comp. Chem*. 26).

IBD study

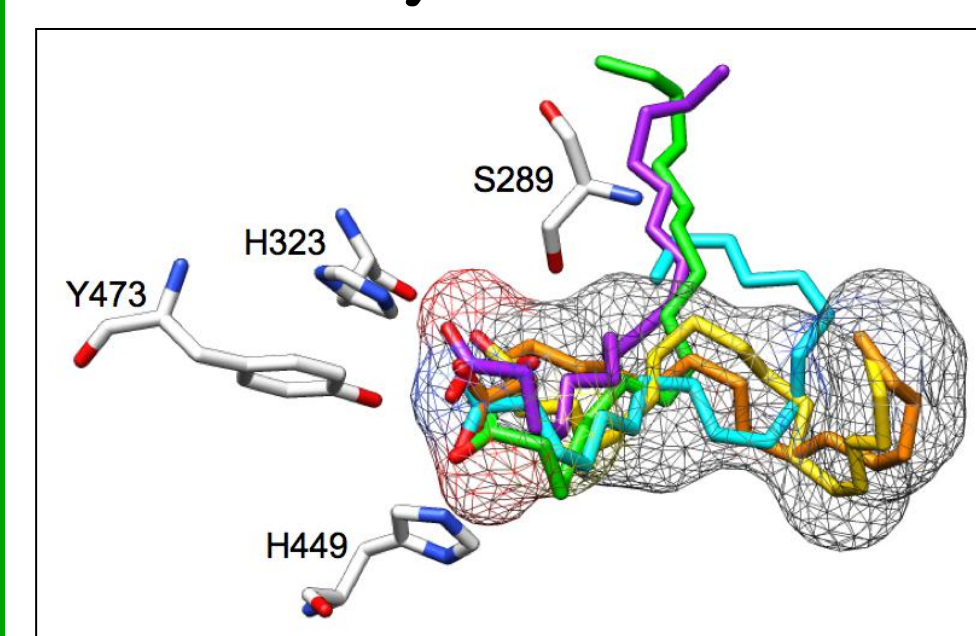
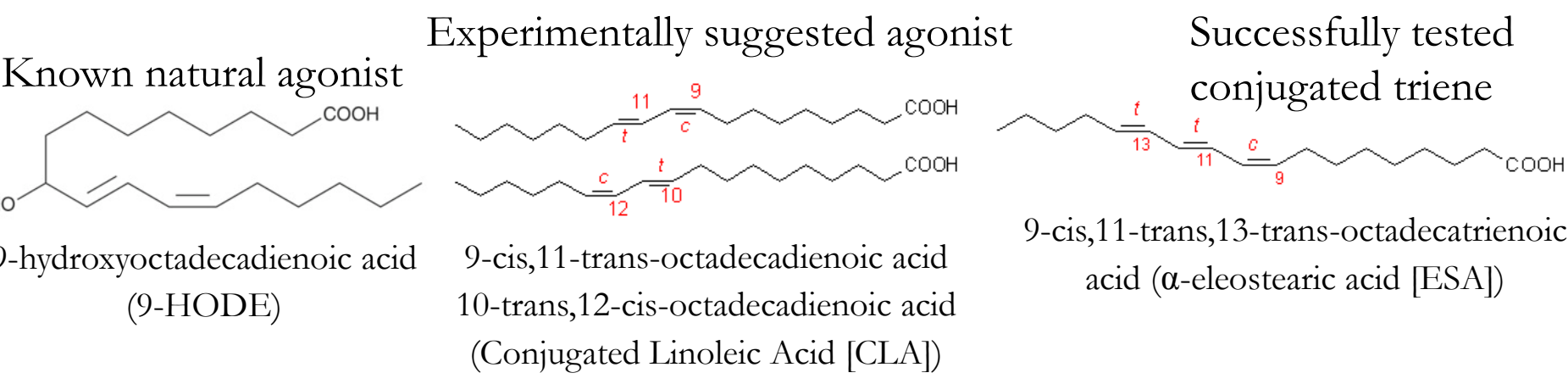


Figure 1 Predicted docked conformations for α -eleostearic (purple), punicic (cyan), calenic (orange), jacaric (green), and catalpic (gold) acids relative to the rosiglitazone-occupied portion of the binding cavity (mesh surface) in the rigid PPAR γ structure model. Key residues with which hydrogen bonding occurs are labeled. Atom-specific coloring: red = oxygen; gray = carbon; blue = nitrogen. Table 1 contains distance measurements for each docked pose. **All tested trienes exhibited agonist-like interactions.**



Ligand	Color	Residue	Distance (Å)	kcal/mol
eleostearic acid	purple	H323.NE2	3.16	-5.6
		Y473.OH	3.01	
		Y473.OH	3.27	
		H449.NE2	2.84	
punicic acid	cyan	Y473.OH	3.03	-4.28
		Y473.OH	3.07	
		H449.NE2	2.81	
		Y473.OH	3.10	
calenic acid	orange	S289.OG	3.05	-4.47
		H323.NE2	3.03	
		Y473.OH	3.26	
		H449.NE2	2.84	
jacaric acid	green	Y473.OH	3.16	-4.5
		Y473.OH	3.10	
		S289.OG	3.02	
		H323.NE2	2.83	
rosiglitazone	gray mesh	H449.NE2	3.02	N/A
		Y473.OH	2.85	

Table 1 Distance measurements (in Angstroms [Å]) suggesting hydrogen bonding for docked conjugated triene poses displayed in Figure 1. Distances were measured between carboxylic oxygen atoms of fatty acids and listed atoms for each residue. Predicted free energy of binding (kcal/mol). Residues are labeled as the amino acid designation plus the atom name (e.g., S289.OG refers to the oxygen atom in the gamma position on serine 289). **ESA exhibited the most favorable binding energy and was used for experimental testing.**

Experimental Methods for IBD study:

- Ligand-binding assay for which fluorescence anisotropy techniques were used to assess the Fluormone depolarization curve for ESA relative to rosiglitazone (positive control). ESA exhibited a curve not significantly different from the positive control.
- Transfection of immortalized mouse precursor macrophages with PPAR γ and luciferase-incorporated plasmids. Introduction of ESA induced luciferase expression similar to levels seen with rosiglitazone.
- Disease and tissue scores were assessed (phenotype effects). PPAR γ -null mice lacked functional protein in colon epithelial and immune cells only.
- Full details and results for this study are in a manuscript currently under review for publication.** Other techniques: immunophenotyping with flow cytometry and quantitative real-time PCR.

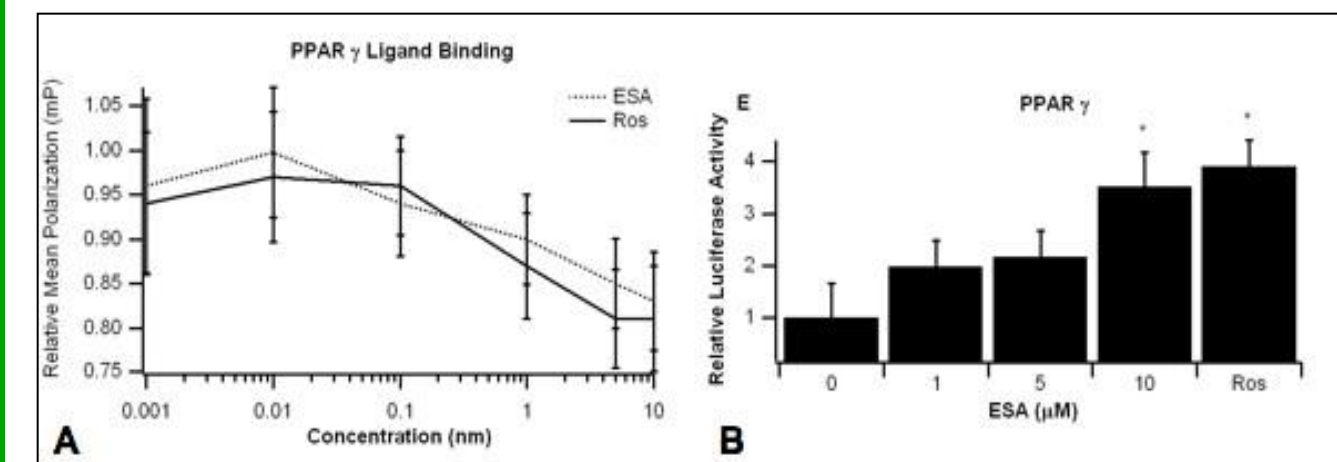


Figure 2 Ligand-binding (A) and reporter assay (B) results for ESA bound to PPAR γ with rosiglitazone (Ros) as a positive control. (A) Ligand binding was assessed as a measure of mean polarization for the displaced Fluormone molecule versus increasing concentrations of each ligand. (B) PPAR γ activation was measured as relative luciferase activity for various concentrations of ESA versus 1 μ M Ros. Error bars represent standard deviation, while asterisks (*) indicate significance ($p \leq 0.05$). **ESA, which was selected as the most favorable compound found in docking, did exhibit agonist-like binding and activity modulation.**

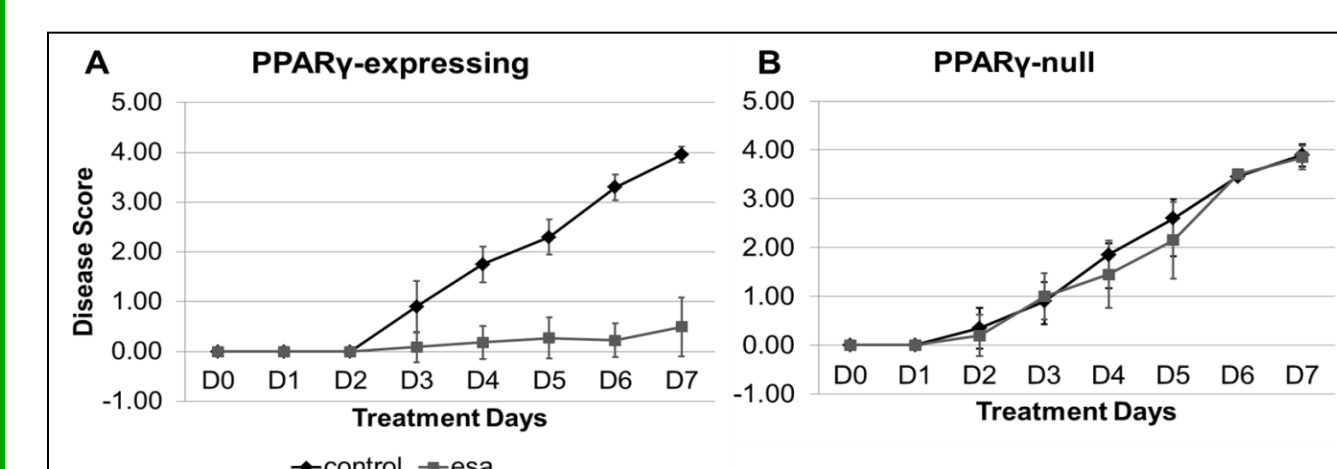


Figure 3 Disease scores for PPAR γ -expressing (A) and PPAR γ -null (B) mice exhibiting DSS-induced IBD over the 7-day treatment period. Data points represent averaged disease scores for each group with error bars representing standard deviation. **ESA reduced disease phenotypes.**

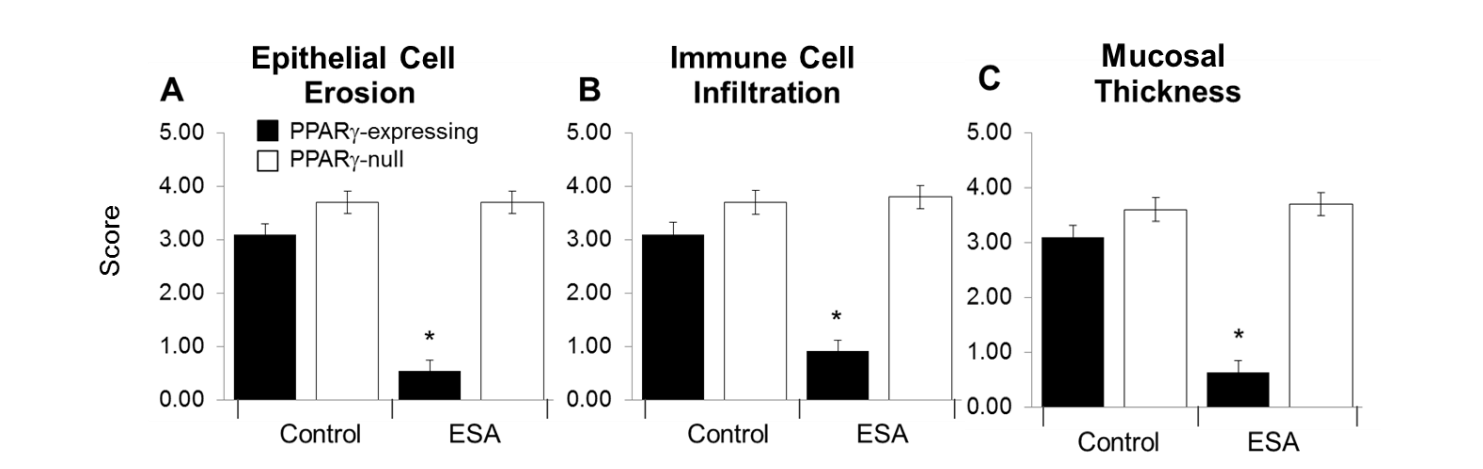
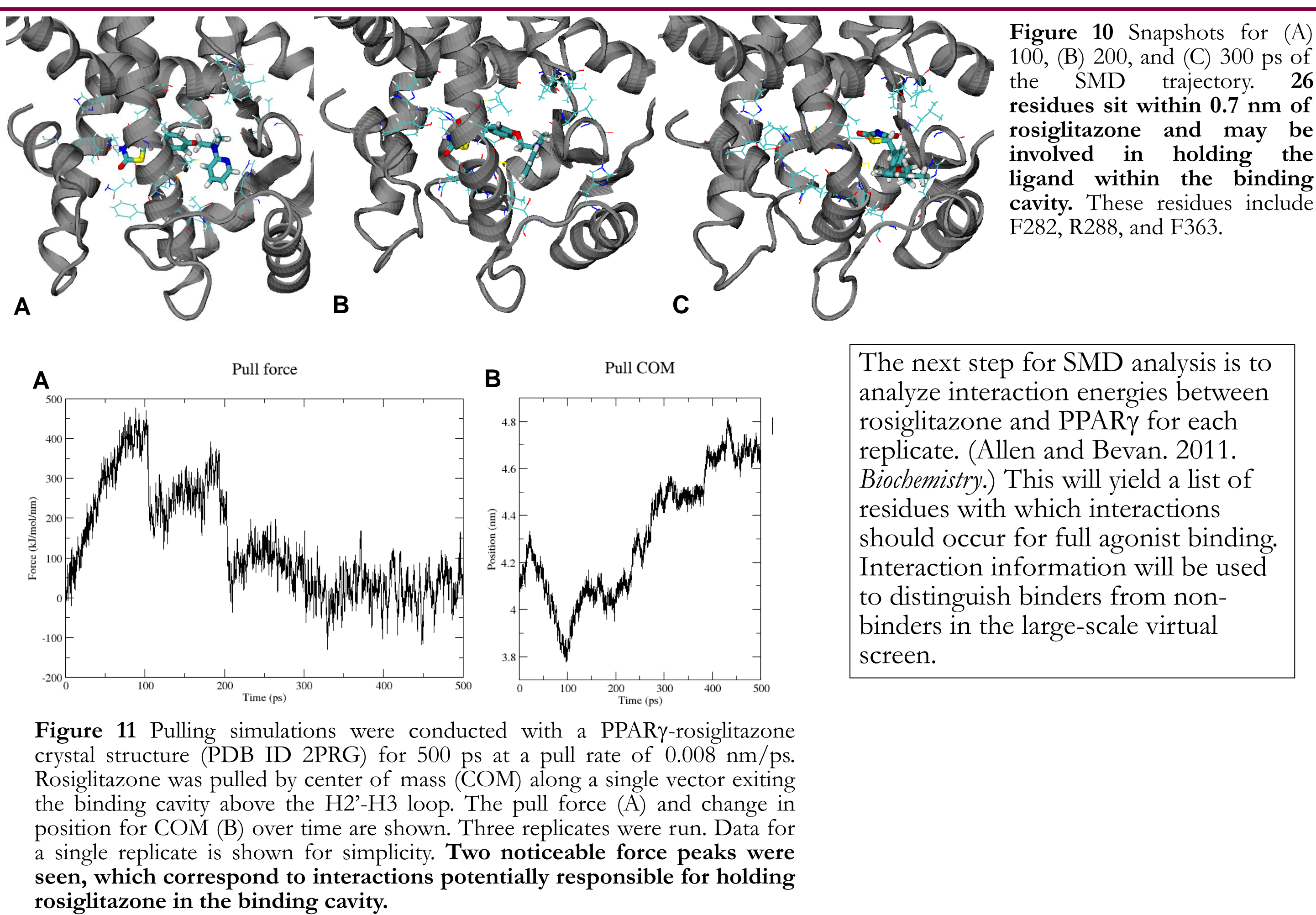


Figure 4 Histology results for DSS-induced IBD under two diets. Epithelial erosion (A), immune cell infiltration (B), and mucosal thickness (C) were assessed and averaged for all the DSS-challenge samples. Asterisk (*) indicates significance ($p \leq 0.05$). **Peripherally, ESA improved upon these phenotypes.**



The next step for SMD analysis is to analyze interaction energies between rosiglitazone and PPAR γ for each replicate. (Allen and Bevan. 2011. *Biochemistry*.) This will yield a list of residues with which interactions should occur for full agonist binding. Interaction information will be used to distinguish binders from non-binders in the large-scale virtual screen.

Ligand-Based Pharmacophores (with examples)

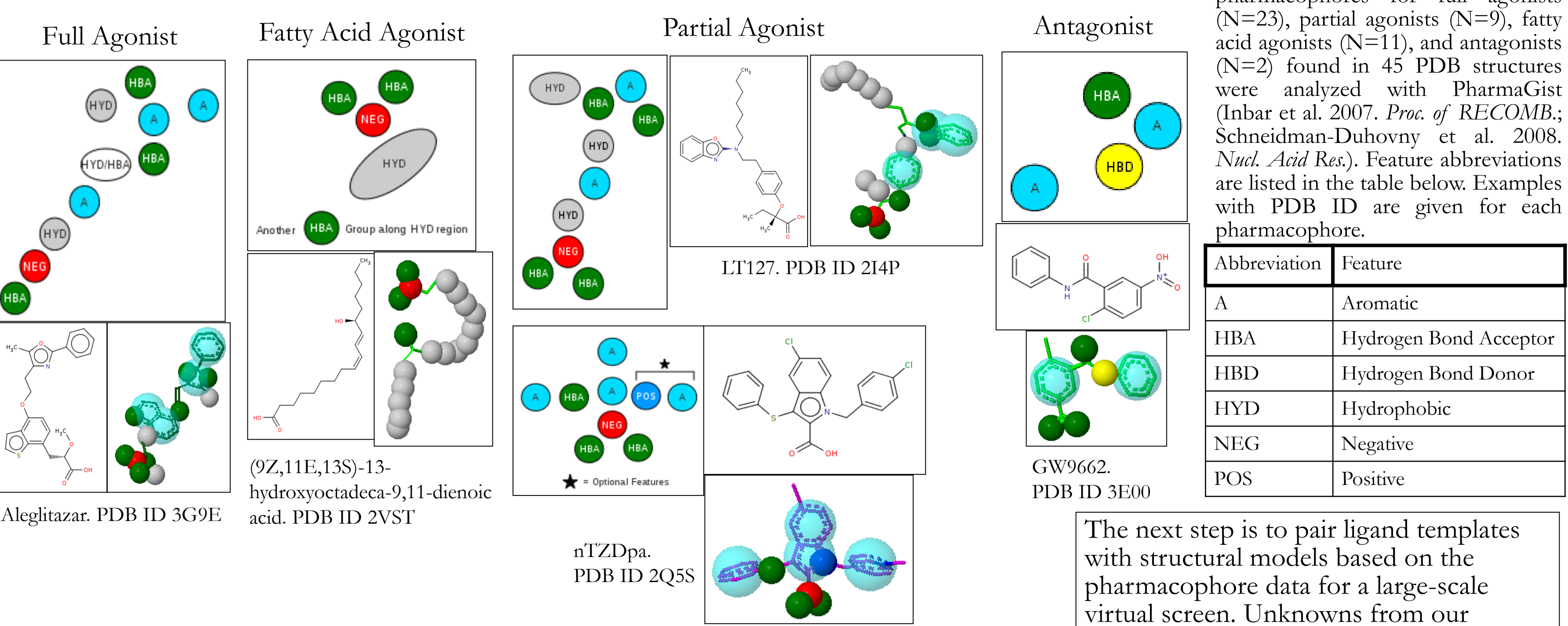


Figure 5 Ligand-based pharmacophores for full agonists (N=23), partial agonists (N=9), fatty acid agonists (N=11), and antagonists (N=2) found in 45 PDB structures were analyzed with PharmaGist (Inbar et al. 2007. *Proc. of RECOMB*.; Schneidman-Duhovny et al. 2008. *Natl. Acad. Res.*). Feature abbreviations are listed in the table below. Examples with PDB ID are given for each pharmacophore.

Abbreviation	Feature
A	Aromatic
HBA	Hydrogen Bond Acceptor
HBD	Hydrogen Bond Donor
HYD	Hydrophobic
NEG	Negative
POS	Positive

The next step is to pair ligand templates with structural models based on the pharmacophore data for a large-scale virtual screen. Unknowns from our database of over 3,000 compounds will be divided according to template and docked. This procedure should reduce false negatives.

Structure-Based Pharmacophores

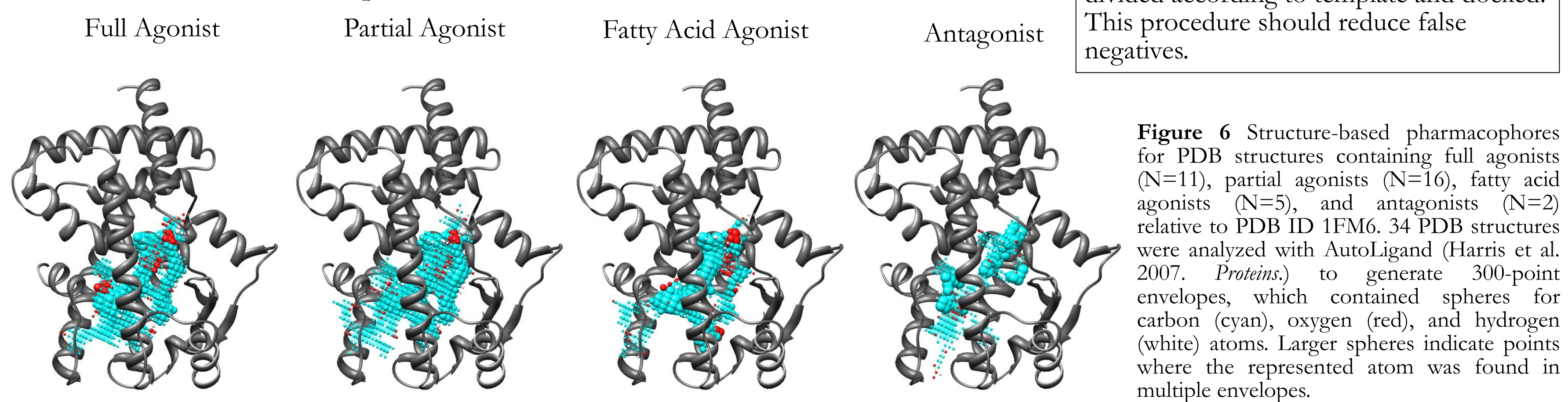


Figure 6 Structure-based pharmacophores for PDB structures containing full agonists (N=11), partial agonists (N=10), fatty acid agonists (N=5), and antagonists (N=2) relative to PDB ID 1FM6. 34 PDB structures were analyzed with AutoLigand (Harris et al. 2007. *Proteins*.) to generate 300-point envelopes, which contained spheres for carbon (cyan), oxygen (red), and hydrogen (white) atoms. Larger spheres indicate points where the represented atom was found in multiple envelopes.

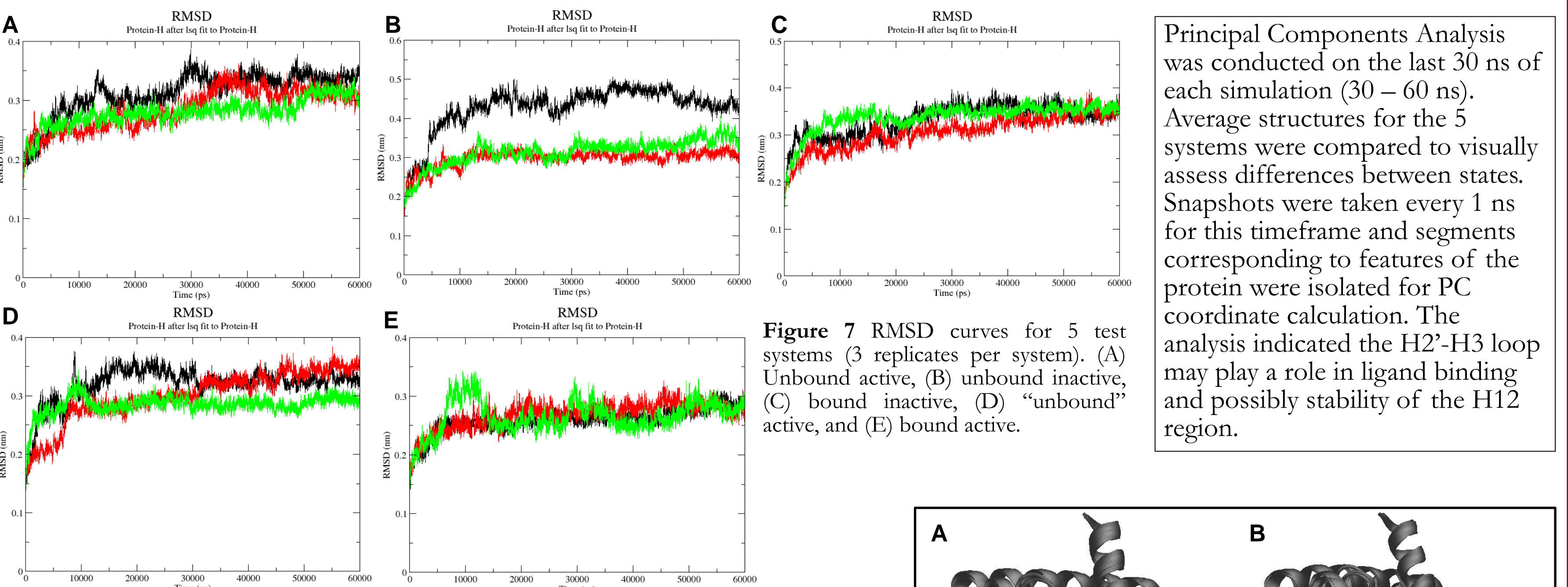


Figure 7 RMSD curves for 5 test systems (3 replicates per system). (A) Unbound active, (B) unbound inactive, (C) bound inactive, (D) "unbound" active, and (E) bound active.

Principal Components Analysis was conducted on the last 30 ns of each simulation (30 – 60 ns). Average structures for the 5 systems were compared to visually assess differences between states. Snapshots were taken every 1 ns for this timeframe and segments corresponding to features of the protein were isolated for PC coordinate calculation. The analysis indicated the H2'-H3 loop may play a role in ligand binding and possibly stability of the H12 region.

Principal Components (PC) Coordinates for H2'-H3 loop

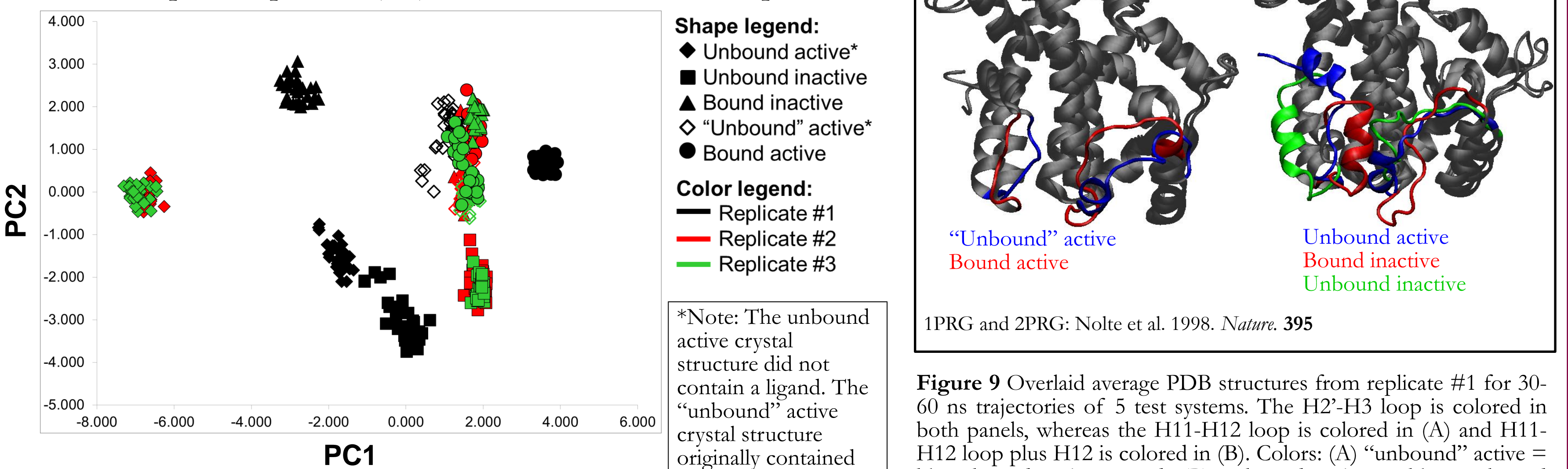


Figure 8 Comparison of first and second principal components for H2'-H3 loop of test systems. Distinctions in movement can be made between systems when segments of the protein are analyzed as isolated units.

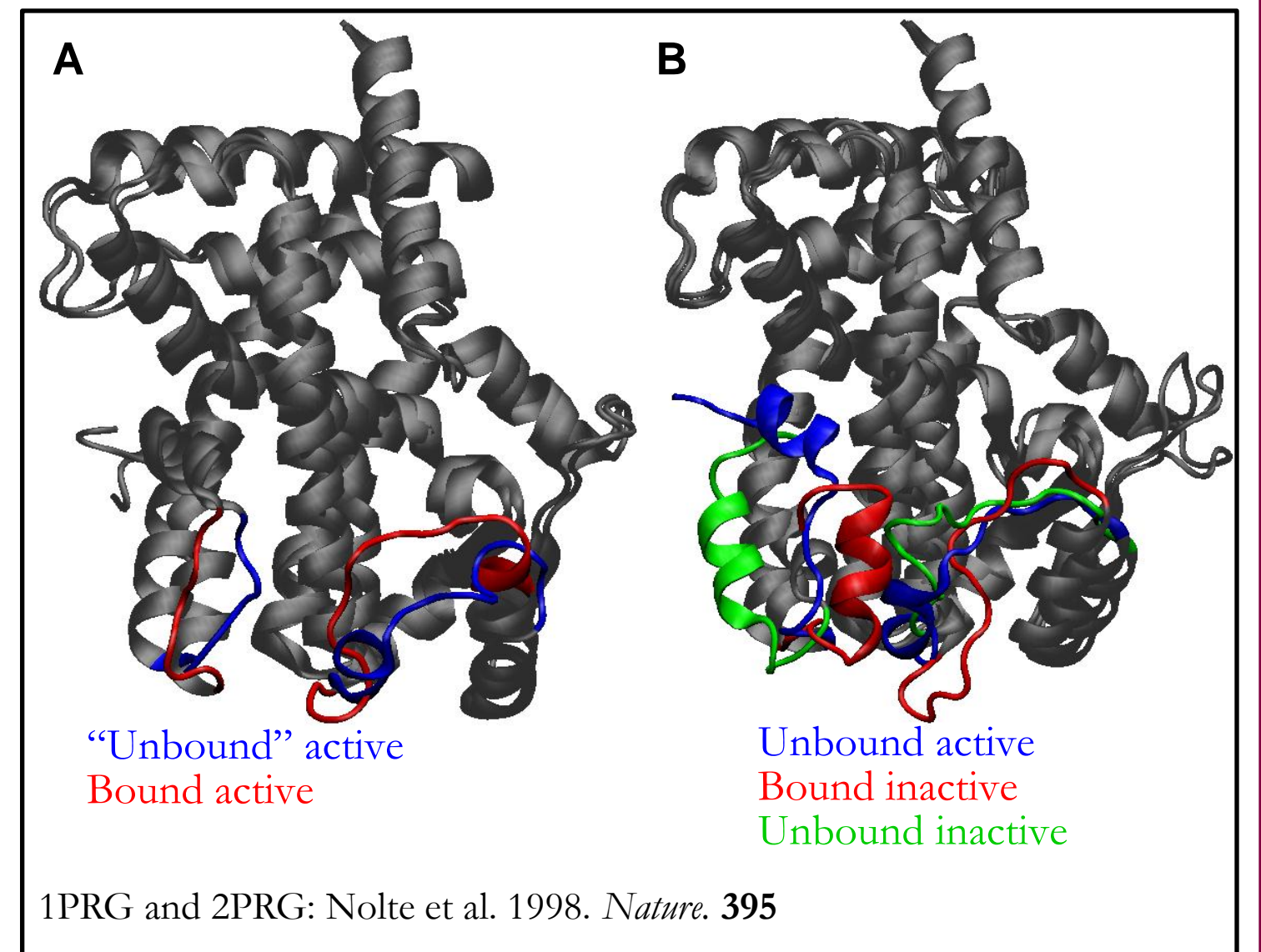


Figure 9 Overlaid average PDB structures from replicate #1 for 30-60 ns trajectories of 5 test systems. The H2'-H3 loop is colored in both panels, whereas the H11-H12 loop is colored in (A) and H11-H12 loop plus H12 is colored in (B). Colors: (A) "unbound" active = blue; bound active = red; (B) unbound active = blue; unbound inactive = green; bound inactive = red. The major correlated components of motion were observed for these regions compared to the remainder of the protein structure.

Acknowledgments

Justin Lemkul, Department of Biochemistry; Dr. William Allen, Stony Brook University The Virginia Tech Advance Research Computing group (VT-ARC) NIH grant 1F31DK091186-01A1 will be used to fund continuation of this project.